



Title	Synthesis of Sc sulfides by CS <sub>2</sub> sulfurization
Author(s)	Kaneko, Takumi; Yashima, Yuta; Ahmadi, Eltefat; Natsui, Shungo; Suzuki, Ryosuke O.
Citation	Journal of solid state chemistry, 285, 121268 <a href="https://doi.org/10.1016/j.jssc.2020.121268">https://doi.org/10.1016/j.jssc.2020.121268</a>
Issue Date	2020-05
Doc URL	<a href="http://hdl.handle.net/2115/84425">http://hdl.handle.net/2115/84425</a>
Rights	©2020. This manuscript version is made available under the CC-BY-NC-ND 4.0 license <a href="https://creativecommons.org/licenses/by-nc-nd/4.0/">https://creativecommons.org/licenses/by-nc-nd/4.0/</a>
Rights(URL)	<a href="http://creativecommons.org/licenses/by-nc-nd/4.0/">http://creativecommons.org/licenses/by-nc-nd/4.0/</a>
Type	article (author version)
File Information	KanekoYashimaAhmadiNatsuiROSuzukiverR2clean.pdf



[Instructions for use](#)

# Synthesis of Sc sulfides by CS<sub>2</sub> sulfurization

Takumi KANEKO <sup>1,\*</sup>, Yuta YASHIMA <sup>1,2</sup>, Eltefat AHMADI <sup>1,3</sup>, Shungo NATSUI <sup>1,4</sup>,  
and Ryosuke O. SUZUKI <sup>1,\*</sup>

<sup>1</sup> Division of Materials Science and Engineering, Faculty of Engineering, Hokkaido  
University, Kita-3, Nishi-8, Kita-ku, Sapporo, Hokkaido 060-8628 Japan

<sup>2</sup> JR East, Shinagawa, Tokyo, Japan

<sup>3</sup> Japan Society for the Promotion of Science (JSPS), 5-3-1 Kojimachi, Chiyoda-ku, Tokyo  
102-0083, Japan

<sup>4</sup> Institute of Multidisciplinary Research for Advanced Materials, Tohoku University, Sendai,  
Japan

<sup>1, \*</sup> corresponding author, tkmknk@eis.hokudai.ac.jp and rsuzuki@eng.hokudai.ac.jp

## Abstract

Scandium sulfides were synthesized from its stable oxide, Sc<sub>2</sub>O<sub>3</sub>, using CS<sub>2</sub> gas. Suitable temperature and time for synthesis were examined experimentally using a constant flow rate of gas mixture of Ar and CS<sub>2</sub>. The high rate of evaporation from liquid CS<sub>2</sub> enhanced formation and stoichiometry of sulfides, and eliminated impurity carbon. Most of parts in the sample were converted to Sc<sub>2</sub>S<sub>3</sub> at 1473 K for 7.2 ks, and a transient phase of Sc<sub>2</sub>O<sub>2</sub>S was often synthesized after a prolonged time under certain oxygen and sulfur potentials.

**Keywords:** synthesis of scandium sulfides, CS<sub>2</sub> gas sulfurization, rare earth compounds, gas-solid reactions

## 26 **1. Introduction**

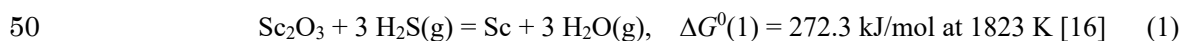
27 In recent years, non-ferrous metallic sulfides have attracted strong attention in various fields,  
28 even if they do not exist as oxide ores in the nature. The sulfides of lithium and titanium have been  
29 studied intensively because of their applications as solid electrolytes in solid state batteries [1,2].  
30  $\text{TiS}_2$  and rare earth sulfides exhibit excellent thermoelectric properties such as low thermal  
31 conductivity and high electric conductivity [3-5], and the materials explore as thermoelectric  
32 elements has been intensively conducted [5-9]. In this study, we focused on scandium sulfide, which  
33 contains one of the rare earth elements.

34 Refining of metal sulfides in molten salts has been recently developed by the authors as an  
35 efficient method for producing metallic powders without oxygen contamination [10-15]. For  
36 example, an industrial grade Ti metal powder has been successfully produced from its oxide,  $\text{TiO}_2$ ,  
37 via titanium sulfides, (i.e.  $\text{Ti}_{2.45}\text{S}_4$  and  $\text{TiS}_2$ ) [14, 15]. Thermodynamically, it is impossible to reduce  
38  $\text{Sc}_2\text{O}_3$ , the most stable metal oxide [16], to metallic Sc directly by Ca because of its strongest affinity  
39 for oxygen [17-19]. However, thermodynamic data indicate that the calciothermic reduction of  
40 scandium sulfide ( $\text{Sc}_2\text{S}_3$ ) may be possible/viable which is due to the different stability of oxide and  
41 sulfides of scandium.

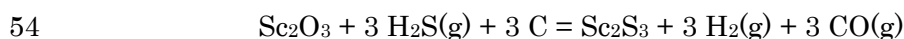
42 Several methods for synthesis of scandium sulfide from the oxide have been known [20-22]. The  
43 first method is direct reaction between metallic scandium and elemental sulfur in an encapsulated  
44 quartz ampoule [20]. In this method a highly pure sulfide of scandium can be synthesized, although

45 scandium metal powder is extremely expensive, and the amount of obtained sulfide is limited.  
46 Therefore, it is desirable to synthesis  $\text{Sc}_2\text{S}_3$  directly from  $\text{Sc}_2\text{O}_3$  rather than serving an expensive  
47 scandium metal as a starting material.

48 The second method is sulfurization of  $\text{Sc}_2\text{O}_3$  in the gas flow of hydrogen sulfide ( $\text{H}_2\text{S}$ ) using a  
49 graphite crucible at 1823 K [21].



51  $\Delta G^0(1)$  is Gibbs free energy change for the reaction (1). Indeed, the reaction between  $\text{Sc}_2\text{O}_3$  and  $\text{H}_2\text{S}$   
52 gas is thermodynamically unfavorable [16] and a contribution of carbon may be required to obtain  
53  $\text{Sc}_2\text{S}_3$  as product.



56 When both carbon and gaseous  $\text{H}_2\text{S}$  are simultaneously used in the process, the sulfurization can  
57 occur because strong reducibility of carbon is preferentially utilized. This may, however, decrease  
58 the reaction efficiency by large amount of  $\text{H}_2\text{S}$  consumption.

59 The sulfurization of  $\text{Sc}_2\text{O}_3$  using gas mixture of  $\text{Cl}_2$  and  $\text{S}_2\text{Cl}_2$  was briefly reported [22], but the  
60 coexisted  $\text{ScCl}_3$  should be additionally converted using  $\text{H}_2\text{S}$  gas and sublimation to obtain pure  $\text{Sc}_2\text{S}_3$ .  
61 No additional report has been found since 1930.

62 On the other hand,  $\text{CS}_2$  gas can be easily used for sulfurization of oxides. It has been reported

63 that stable oxides such as  $\text{TiO}_2$  can be converted to  $\text{TiS}_2$  in  $\text{CS}_2$  gas [5,13,15]. Silicon sulfide and rare  
64 earth sulfides have been also successfully synthesized in a  $\text{CS}_2$  gas atmosphere [23-26].  $\text{CS}_2$  gas can  
65 serve carbon and sulfur simultaneously with a stoichiometric molar ratio, and react with  $\text{Sc}_2\text{O}_3$  due  
66 to its strong thermochemical reducibility and sulfurization ability. The overall sulfurization reaction  
67 can be written apparently as reaction (3),



$$69 \quad \Delta G^0(3) = -42.8 \text{ kJ/mol at } 1473 \text{ K, and } -40.5 \text{ kJ/mol at } 1273 \text{ K [16]} \quad (3)$$

70 where an inert gas such as Ar is used to transport the vaporized sulfurizing agent ( $\text{CS}_2$  gas) into the  
71 reaction vessel. This can be performed by injecting an inert gas into liquid  $\text{CS}_2$  and vaporizing  $\text{CS}_2$  at  
72 room temperature, for example.

73 The boiling point of  $\text{CS}_2$  is as low as 315 K [16], and it can be easily handled and fed into the  
74 reaction vessel rather than elemental sulfur which is solid at ambient temperature. It is worth noting  
75 that the melting temperature of sulfur is 388.4 K [16], and that the evaporation requires an additional  
76 furnace to keep a constant temperature above 473 K [17]. Moreover, the excess  $\text{CS}_2$  gas can be  
77 collected by cooling due to its very low boiling point. The  $\text{CS}_2$  gas is commonly used as a solvent for  
78 organic materials. A constant supply of  $\text{CS}_2$  at a reasonable cost is desired for the sulfurization  
79 process (reaction (3)). No literature survey is available on the preparation of  $\text{Sc}_2\text{S}_3$  from  $\text{Sc}_2\text{O}_3$  as far  
80 as the authors are aware.

81  $\text{Sc}_2\text{S}_3$  has a potential as sulfide-based solid electrolyte for fuel cells and as new thermoelectric  
82 materials, similar to the other rare-earth sulfides [1-9]. Because  $\text{Sc}_2\text{S}_3$  has a characteristically bright  
83 yellow color, it can be expected to be used as a yellow pigment [20-22] and as n-type  
84 semi-conductor [20] for optical application. The authors are expecting that  $\text{Sc}_2\text{S}_3$  can be a starting  
85 material for scandium metal production.

86 The purpose of this paper is to synthesize  $\text{Sc}_2\text{S}_3$  from  $\text{Sc}_2\text{O}_3$  by employing  $\text{CS}_2$  gas as powerful  
87 sulfurizing agent. This paper studies the optimal evaporation temperature of  $\text{CS}_2$  gas as well as  
88 sulfurization temperature to form the single phase of  $\text{Sc}_2\text{S}_3$ . Morphology of the sulfurized samples  
89 was also rigorously investigated.

90

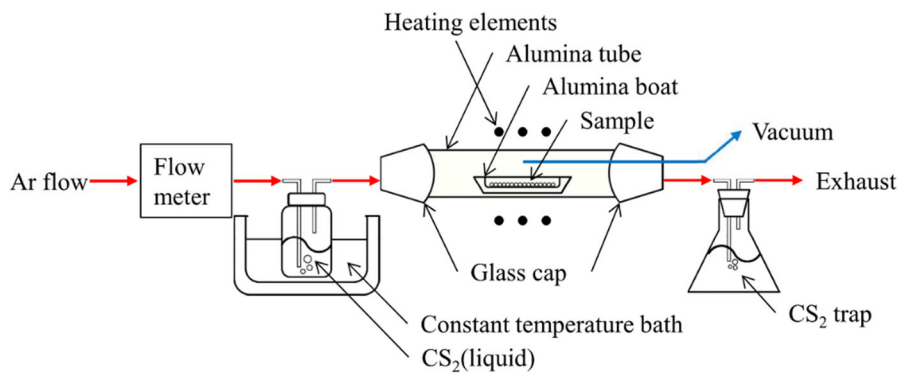
## 91 **2. Experimental procedure**

### 92 **2.1 Materials and experimental setup**

93  $\text{Sc}_2\text{O}_3$  powder with the purity of 99.9% was supplied by Sumitomo Metal Mining Co., Ltd. Fig. 1  
94 shows the experimental setup [13]. The vapor pressure of volatile  $\text{CS}_2$  (99.99%, Wako Chemical  
95 Co.) is so high even at room temperature that it can be fed to the hot reaction zone by a constant flow  
96 of Ar gas (>99.9998%, 20 mL/min.). The evaporation temperature of  $\text{CS}_2$  gas was kept constant by  
97 water bath. A dense alumina tube (24 mm ID) was used as a reaction tube, and unreacted exhaust gas  
98 was trapped by using 1.0 M NaOH solution. In the sulfurization experiment, 0.25 g of the  $\text{Sc}_2\text{O}_3$  was

99 weighted and filled into an alumina boat (>99.5%, 14mm wide, 100 mm long). The sample was  
100 heated in vacuum up to the sulfurization temperature. Then, a mixture of Ar and CS<sub>2</sub> gas was served  
101 for the sulfurization. The sulfurization temperature was varied in the range between 1273 K and  
102 1473 K, and both the heating and cooling rates were 10 K/min. After cooling, the mass changes of  
103 the samples were precisely measured to estimate the sulfurization degree of the samples.

104



105

106

Fig.1 A schematic illustration of the experimental setup.

107

## 108 2.2 Characterization

109

110

111

112

113

114

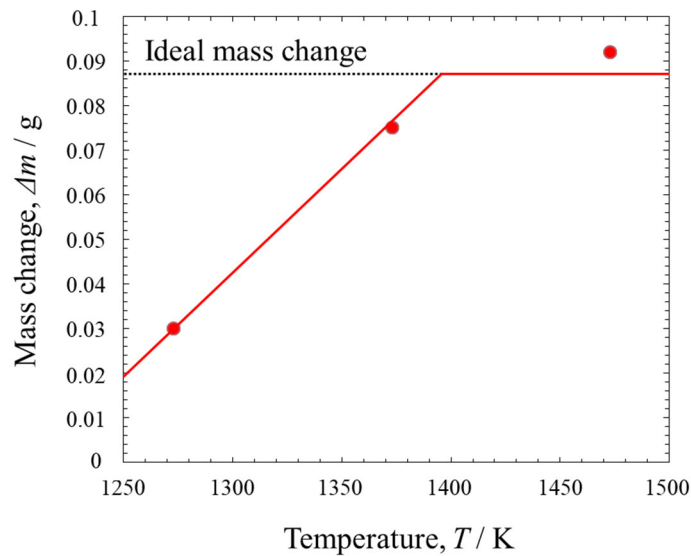
115

The samples were analyzed by X-ray diffraction (XRD) measurement using Philips X'Pert Pro, (Cu-K<sub>α</sub>). The morphology of as-received and the sulfides of scandium were characterized by scanning electron microscopy (SEM, JSM-6510LA). The carbon and sulfur concentrations in the obtained samples were quantitatively analyzed by the IR spectroscopic analysis of CO<sub>2</sub> and SO<sub>2</sub> gases, respectively, using LECO CS-600. The oxygen concentration was also analyzed by the inert-gas fusion method using LECO TC-600.

### 116 3. Results and discussion

#### 117 3.1 Optimal reaction temperature and time

118 The optimal sulfurization temperature and time suitable for formation of  $\text{Sc}_2\text{S}_3$  from  $\text{Sc}_2\text{O}_3$  were  
119 examined, where the evaporation temperature of  $\text{CS}_2$  was set constant at 273 K. Fig. 2 shows the  
120 mass change ( $\Delta m$ ) of the sulfurized samples at temperatures ranged from 1273 K and 1473 K for 7.2  
121 ks. At 1473 K, the mass change ( $\Delta m$ ) was close to the ideal mass gain from  $\text{Sc}_2\text{O}_3$  to  $\text{Sc}_2\text{S}_3$ . It is  
122 noted that the sufficient amount of  $\text{CS}_2$  was supplied in the experiment, the amount of sulfur in the  
123 consumed  $\text{CS}_2$  gas in 7.2 ks was 21.5 times more that the stoichiometric sulfur required for  
124 formation of  $\text{Sc}_2\text{S}_3$  in conversion of  $\text{Sc}_2\text{O}_3$  perfectly to  $\text{Sc}_2\text{S}_3$  at the operating conditions.



125

126

Fig.2 Mass change after  $\text{CS}_2$  gas sulfurization for 7.2 ks.

127

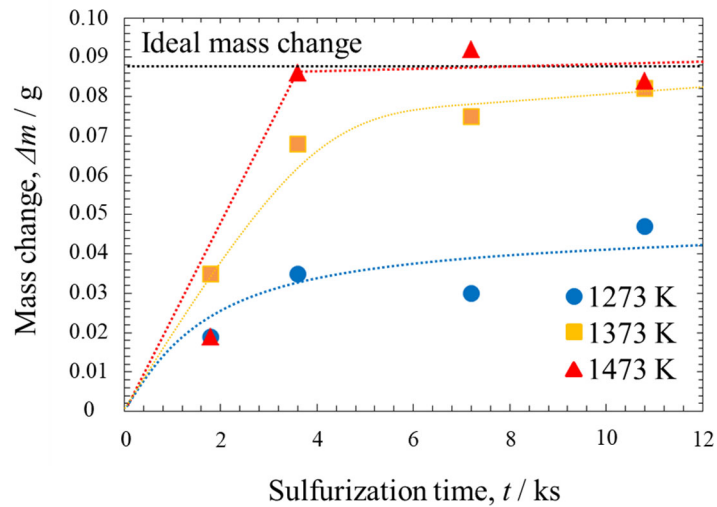
128

129

Fig.3 shows the time dependency of mass changes of the samples. The mass changes were smaller than the ideal value at all the temperatures when the sulfurization time was as short as 1.8 ks.

130 At 1273 K, the mass gradually increased as the time prolonged, however, the mass changes did not  
 131 approach the ideal value for a complete conversion, and it approached about a 1/3 value of the  
 132 expected stoichiometry,  $\text{Sc}_2\text{S}_3$ . At 1373 K, the mass did not arrive to the ideal mass for the shorter  
 133 time such as 3.6 ks and 7.2 ks, but the sample reacted for 10.8 ks showed the ideal mass gain. At  
 134 1473 K, the mass change was close to ideal value of  $\text{Sc}_2\text{S}_3$  even after 3.6 ks, and did not increase  
 135 after 3.6 ks. Thus the sulfurization occurred at a fairly fast rate and it related strongly with the  
 136 operation temperature.

137



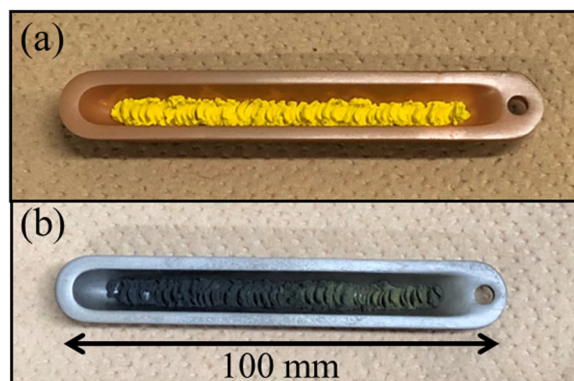
138

139 Fig.3 Mass change after  $\text{CS}_2$  gas sulfurization.

140

141 Fig. 4 shows the appearance of the sample after sulfurization at 1473 K for 7.2 ks. The color as  
 142 shown in Fig.4(a) was bright yellow and slightly sintered, although the starting oxide,  $\text{Sc}_2\text{O}_3$ , is  
 143 white and powdery. The yellow product was easily pulverized by soft finger touching.

144



145

146 Fig.4 Apparent view of sulfurized sample at 1473 K for 7.2 ks. CS<sub>2</sub> liquid was hold at 273 K (a), and  
147 313 K (b).  
148

149

Fig.5 shows the XRD patterns of as-received and the sulfurized samples at various temperatures.

150

After sulfurization for 7.2 ks at the lowest investigated temperature of about 273 K, Sc<sub>2</sub>O<sub>3</sub> (ICSD No.

151

01-073-1691)[27], Sc<sub>2</sub>O<sub>2</sub>S (ICSD No. 01-070-1251)[28-30] and Sc<sub>2</sub>S<sub>3</sub> (ICSD No. 01-073-0451) [21]

152

were identified in the samples, indicating the formation of Sc<sub>2</sub>S<sub>3</sub> through an intermediate oxysulfide

153

phase. By increasing the reaction temperature to above 1373 K, the intensities of the XRD peaks

154

associated to oxide and oxysulfide significantly decreased. Further increasing the temperature to

155

1473 K resulted in formation of the sulfide of Sc<sub>2</sub>S<sub>3</sub> with a small amount of Sc<sub>2</sub>O<sub>2</sub>S. A faint amount

156

of Sc<sub>2</sub>O<sub>2</sub>S was still found in the sample prepared at 1473 K for 7.2 ks, although the major phase was

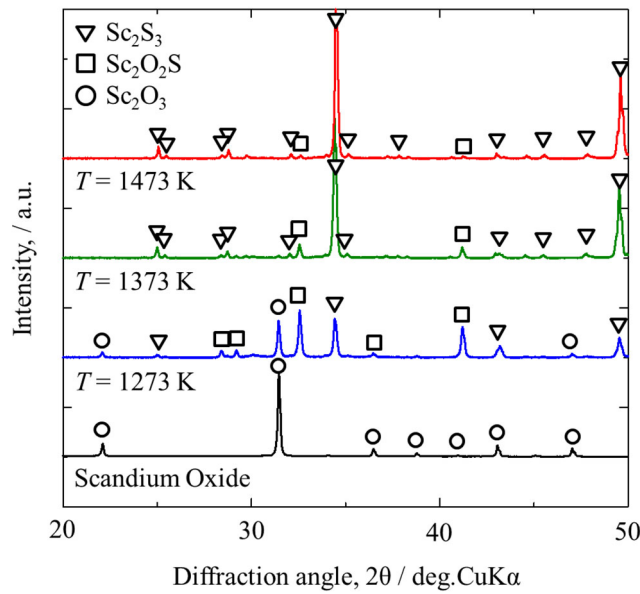
157

Sc<sub>2</sub>S<sub>3</sub> and any diffraction peaks of Sc<sub>2</sub>O<sub>3</sub> was not detected. Thus, the sample synthesized at 1473 K

158

could be considered as nearly single phase of Sc<sub>2</sub>S<sub>3</sub>.

159

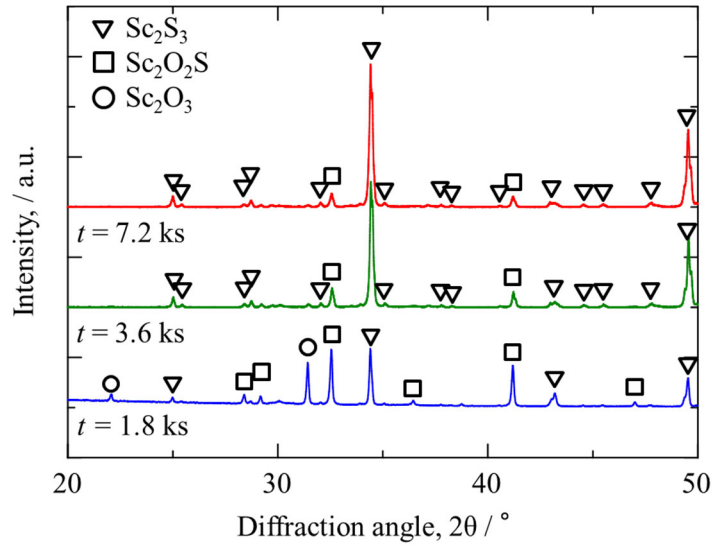


160  
161

162 Fig. 5 X-ray diffraction patterns of the samples sulfurized at various temperatures for 7.2 ks.  
163

164 In addition, the sulfurization experiments were conducted at 1373 K for various periods ranged  
165 from 1.8 ks to 7.2 ks. Fig.6 shows the time dependency of phase transition by XRD patterns at 1373  
166 K. The sample prepared for 1.8 ks contained three phases including  $\text{Sc}_2\text{O}_3$ ,  $\text{Sc}_2\text{O}_2\text{S}$  and  $\text{Sc}_2\text{S}_3$ . After  
167 sulfurization for 3.6 ks, the intensities of the XRD peaks of  $\text{Sc}_2\text{O}_3$  and  $\text{Sc}_2\text{O}_2\text{S}$  decreased and  $\text{Sc}_2\text{S}_3$   
168 became the dominant phase in the product. The XRD patterns of the samples synthesized at 1373 K  
169 in 3.6 ks and 7.2 ks were almost similar, and a slight decrease in intensity of  $\text{Sc}_2\text{O}_2\text{S}$  peaks was  
170 observed. The peaks related to  $\text{Sc}_2\text{O}_3$  were completely disappeared after sulfurization for 3.6 ks and  
171 7.2 ks. This indicates that  $\text{Sc}_2\text{S}_3$  could be synthesized at shorter times.

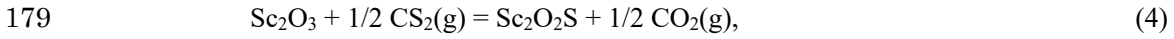
172



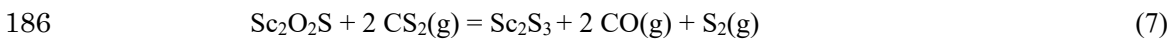
173  
174  
175  
176

Fig.6 X-ray diffraction patterns of the samples sulfurized at 1373 K.

177 These phase identifications indicated that the sulfuration of  $\text{Sc}_2\text{O}_3$  (reaction (3)) proceeds  
178 through the formation of an intermediate oxysulfide,  $\text{Sc}_2\text{O}_2\text{S}$ , that may be explained as follows:



181 Apparently, the replacement of one atom of oxygen in the oxide lattice by sulfur occurs, and the  
182 crystalline oxysulfide of  $\text{Sc}_2\text{O}_2\text{S}$  was then formed. Further substitution of oxygen atoms in  $\text{Sc}_2\text{O}_2\text{S}$   
183 by sulfur results in formation of the most stable sulfide,  $\text{Sc}_2\text{S}_3$ . It is noted that only  $\text{CO}_2$  gas is  
184 considered in the reactions (4) and (26). CO gas can be also considered in the parallel reactions as,



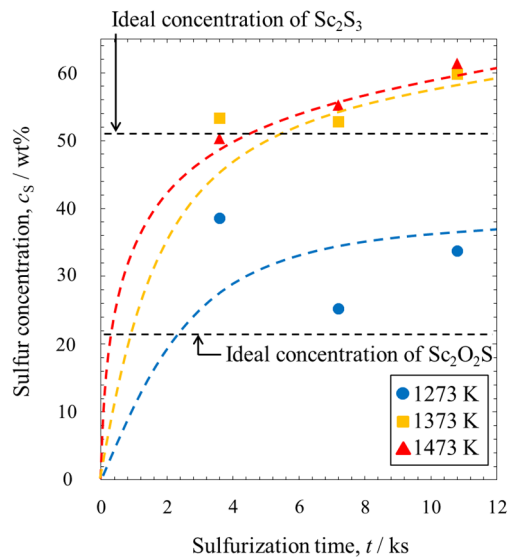
187 The experimental determination of the concentrations of CO and  $\text{CO}_2$  in the gaseous phase is not

188 easy due to the presence of  $S_2$  and the residual  $CS_2$  gases, although it is thermodynamically possible

189 to consider simultaneous formation of CO and  $CO_2$  gases in the reactions (4) – (7).

190

191



192

193

Fig.7 Sulfur content of the sulfurized samples.

194

195 The sulfur contents of the obtained samples were quantitatively analyzed as shown in Fig.7. It

196 should be noted that the stoichiometric  $Sc_2S_3$  contains 51.7 wt%S, however, the highest sulfur

197 content of the sample obtained at 1273 K was about 40 wt%S, which is less than the stoichiometric

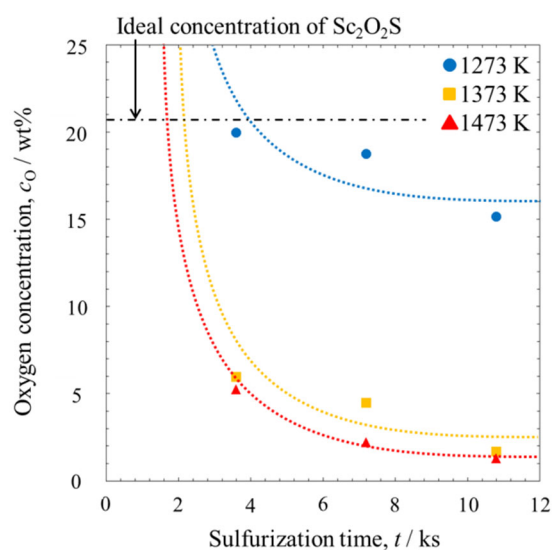
198 sulfur content of  $Sc_2S_3$ . The sulfur concentration of the samples synthesized at 1373 and 1473 K

199 were as high as 51.7 wt%S, even after a short reaction time such as 3.6 ks. The sulfur content of the

200 samples increased as the reaction time became longer. The increase of sulfur content above the

201 stoichiometry may reflect the non-stoichiometry in  $Sc_2S_3$ . The deposition of sulfur vapor on the

202 sample surface during cooling also increases the sample weight, because  $S_2$  gas generates as the  
203 reactions (6) and (7). It is certain that the excess amount of  $CS_2$  gas caused the yellow deposition of  
204 solid sulfur at the cold position of the downstream in the reaction tube.  
205



206  
207  
208  
209

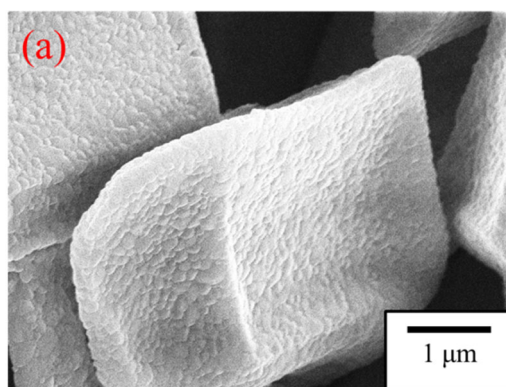
Fig.8 The residual oxygen content of the sulfurized samples.

210 Fig. 8 shows the residual oxygen of the sulfurized samples analyzed by LECO method. Note that  
211 the oxygen concentrations in the stoichiometric oxide  $Sc_2O_3$  and the oxysulfide  $Sc_2O_2S$  are 34.80  
212 wt% and 20.79 wt%, respectively. The oxygen level of the samples sulfurized at 1273 K was very  
213 high, while those at 1373 and 1473 K decreased to a low level. The oxygen concentration at 1473 K  
214 for 10.8 ks was analyzed as 1.31 wt%O as the lowest content. This means that the sulfurization  
215 behavior significantly changed at a critical temperature between 1273 K and 1373K.  
216

### 217 3.2 Microstructural characterization of the products

218 Fig. 9 shows the morphology of as-received oxide and the synthesized samples. As shown in Fig.  
219 9(a), the raw material ( $\text{Sc}_2\text{O}_3$ ) contained larger grains of about  $4\ \mu\text{m}$  and the finer particles of about  
220  $0.1\ \mu\text{m}$ . These oxide particles were then sulfurized at  $1273\ \text{K}$  for  $7.2\ \text{ks}$ . Many cracks were formed in  
221 all the particles as shown in Fig. 9(b), which could be due to lattice mis-fitting between oxide and  
222 oxysulfide. EDX analysis showed the homogeneous distribution of sulfur and oxygen in all the  
223 particles. The oxysulfide particles were formed in hexagonal shape plates as shown in Fig. 9(c). Fig.  
224 9(d) shows the morphology of the sulfide sample prepared at  $1473\ \text{K}$  for  $7.2\ \text{ks}$ . It consists of  
225 hexagonal grains, and they look to grow toward the cylindrical directions accompanying with  
226 non-uniform branches. FE-SEM micrograph of the particles at higher magnification is shown in Fig.  
227 9(e) in which the interconnected hexagonal plates of  $\text{Sc}_2\text{S}_3$  with particle size of about  $50 - 100\ \text{nm}$   
228 can be obviously seen.

229

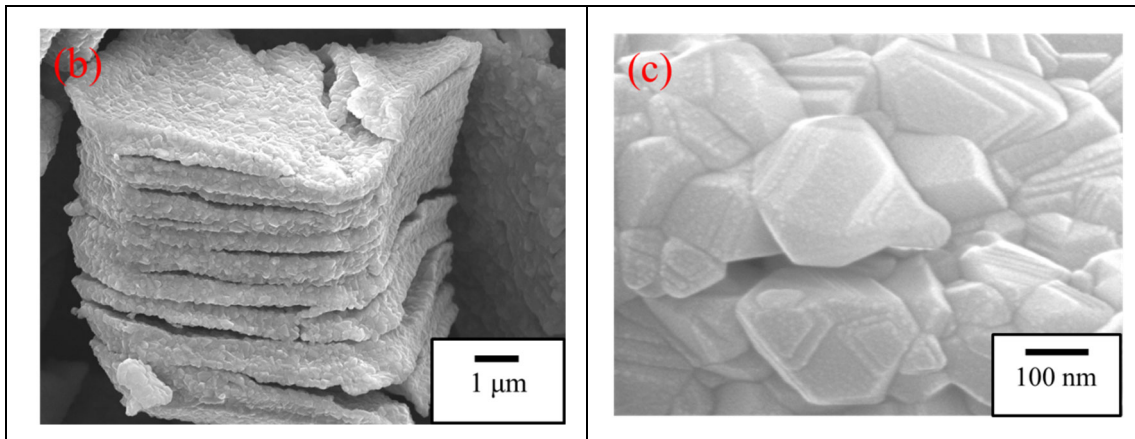


230

231

232

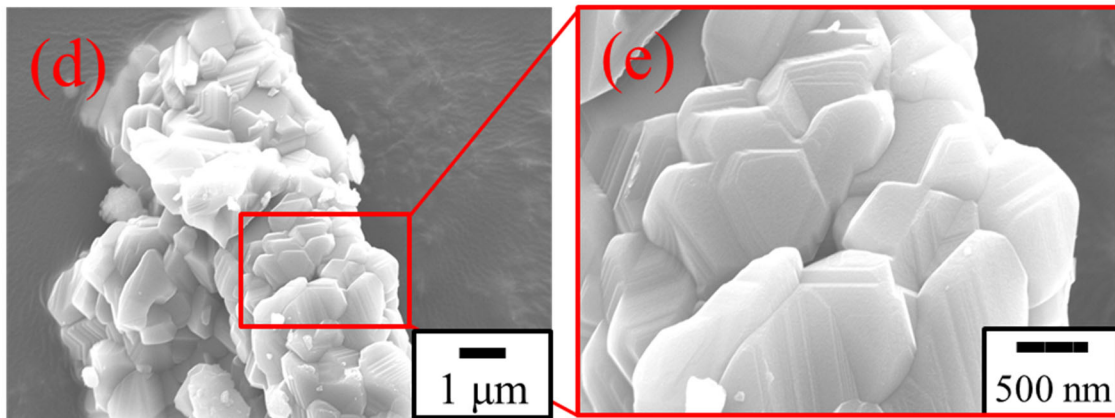
(a)



233

(b)

(c)



234

(d)

(e)

235

236

237 Fig. 9 SEM images of (a) as-received scandium oxide and the synthesized sulfides at 1273 K (b, c),  
 238 and 1473 K (d, e) for 10.8 ks.

239

### 240 3.3 Evaporation temperature of CS<sub>2</sub>

241 Figures 10 and 11 show the mass changes and the oxygen concentration of the samples prepared

242 at various conditions, respectively. Sulfurization of the samples was conducted at various

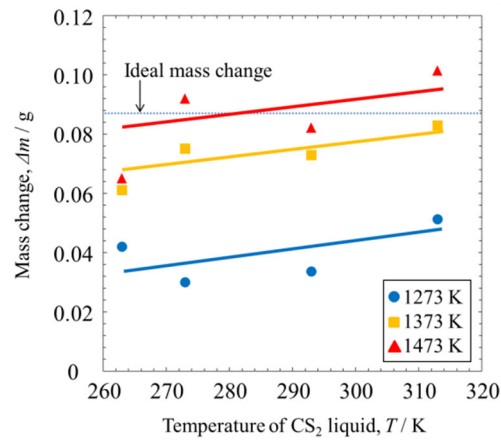
243 temperatures for 7.2 ks, where the evaporation temperature of CS<sub>2</sub> liquid was varied. As the

244 temperature of CS<sub>2</sub> liquid increases, the equilibrium vapor pressure is the higher [16], and the large

245 amount of CS<sub>2</sub> gas is supplied into the hot zone of the furnace. The mass changes of the samples

246 increased due to the substitution of oxygen atoms by sulfur. The residual oxygen also changed as the  
 247 temperature of CS<sub>2</sub> liquid varied, as shown in Fig.11.

248

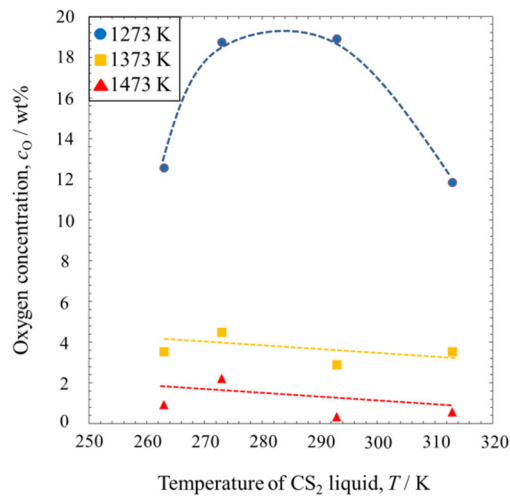


249

250

251 Fig.10 Mass change of sulfurized samples for 7.2 ks at various CS<sub>2</sub> evaporation temperatures.

252



253

254 Fig. 11 Oxygen concentration of the sulfurized samples for 7.2 ks at various CS<sub>2</sub> evaporation  
 255 temperatures.

256

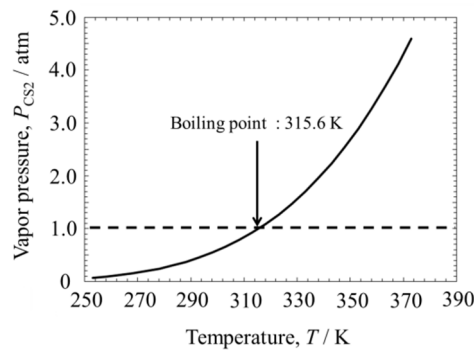
257 When CS<sub>2</sub> gas is in equilibrium with its pure liquid as given in eq. (8), its vapor pressure can be

258 thermodynamically determined as a function of temperature as written in eq. (9). The standard Gibbs

259 free energy change for the reaction (8),  $\Delta G^0(8)$  [16], is used to evaluate the vapor pressure of  $\text{CS}_2$ ,  
 260  $P_{\text{CS}_2}$ , as shown in Fig. 12. The  $\text{CS}_2$  gas at  $P_{\text{CS}_2}$  was supplied to the reaction zone and it was  
 261 apparently reacted with  $\text{Sc}_2\text{O}_3$  to form  $\text{Sc}_2\text{S}_3$  (reaction (3)), although it consisted of two stepwise  
 262 reactions, (2)-(5).



$$P_{\text{CS}_2} = \exp\left(\frac{-\Delta G^0(8)}{RT}\right) \quad (9)$$



265 Fig.12 Vapor pressure of  $\text{CS}_2$  vs evaporation temperature [16].

267 When the higher  $P_{\text{CS}_2}$  is given by increasing the evaporation temperature of  $\text{CS}_2$  liquid, the  
 268 sulfurization can be thermodynamically enhanced. Assuming the coexistence of pure  $\text{Sc}_2\text{O}_3$  and pure  
 269  $\text{Sc}_2\text{S}_3$  as represented in reaction (3), the Gibbs free energy change of sulfurization,  $\Delta G(3)$ , can be  
 270 written as eq. (10),

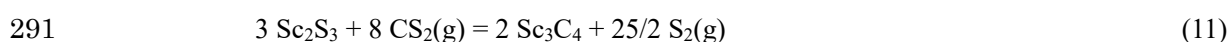
$$\Delta G(3) = \Delta G^0(3) + \frac{3}{2}RT \ln P_{\text{CO}_2} - \frac{3}{2}RT \ln P_{\text{CS}_2} \quad (10)$$

271  
 272  
 273  $P_{\text{CS}_2}$  can be given in eq.(9) as determined by the holding temperature of  $\text{CS}_2$  liquid. On the other

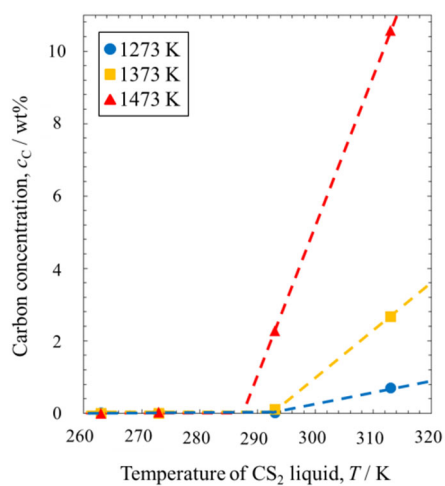
274 hand,  $P_{\text{CO}_2}$  is limited by the mass balance of charged amount of  $\text{Sc}_2\text{O}_3$ . Because  $\text{CO}_2$  gas is diluted  
275 by carrier gas of Ar,  $P_{\text{CO}_2}$  gradually decreases after completing the reaction. If we can assume  $P_{\text{CO}_2}$  is  
276 nearly constant, the increase of holding temperature of  $\text{CS}_2$  liquid increases  $P_{\text{CS}_2}$ , and  $\Delta G(3)$  can  
277 shift to the more negative value according to eq.(10). This enhancement of reaction lowers the  
278 residual oxygen content in the sulfide due to decomposition of oxide.

279 However, the specimens changed the color to black as shown in Fig. 4(b) when they were  
280 sulfurized by  $\text{CS}_2$  gas evaporated at the holding temperature of  $\text{CS}_2$  liquid as high as 313 K. Fig. 13  
281 shows the residual carbon in the samples sulfurized for 7.2 ks. The black sample at 1473 K using  
282  $\text{CS}_2$  gas evaporated at 313 K was heavily contaminated with carbon (10.6 wt%C at the maximum),  
283 and the faint diffraction peaks matched with those of  $\text{Sc}_{15}\text{C}_{19}$  (ICSD#00-038-0797) [30-32] among  
284 many Sc carbides [30-42], as shown in Fig. 14. It is noted that the chemical formula was reported  
285 earlier as  $\text{Sc}_{15}\text{C}_{19}$  [30-32], and that it was revised as  $\text{Sc}_3\text{C}_4$  by neutron diffraction measurements  
286 [39-42]. Hereafter we call  $\text{Sc}_{15}\text{C}_{19}$  as  $\text{Sc}_3\text{C}_4$ . It was reported that the color of  $\text{Sc}_3\text{C}_4$  crystal is a light  
287 gray with metallic luster, and the powdered sample is black [39]. The color changes are in agreement  
288 with this study.

289 Because the excess amount of  $\text{CS}_2$  gas was fed to the sample,  $\text{S}_2$  gas and  $\text{Sc}_3\text{C}_4$  are produced  
290 from the decomposition of  $\text{CS}_2$  gas.

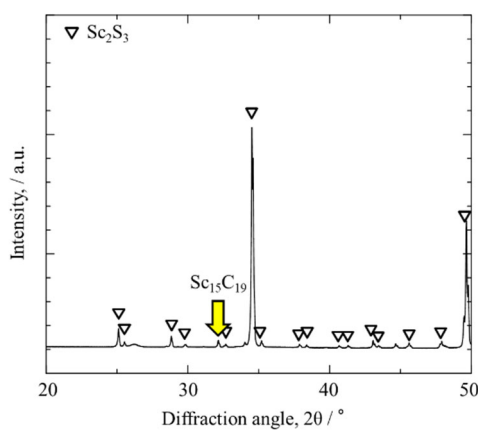


292 The deposited carbon dissolves into sulfide, and a portion of carbon forms the carbide such as  $\text{Sc}_3\text{C}_4$   
 293 when the amount of deposition exceeds the solubility of carbon. Because neither thermodynamic  
 294 data on scandium carbides nor phase relationship among sulfides and carbides are available, the  
 295 exact evaluation on eq. (11) can not be completed.  
 296



297  
 298  
 299  
 300

Fig.13 Carbon content of the samples prepared by evaporation of CS<sub>2</sub> at various temperatures.



301  
 302

303 Fig.14 XRD pattern of sulfurized sample at 1473 K for 7.2 ks by using CS<sub>2</sub> gas evaporated at 313 K.

304

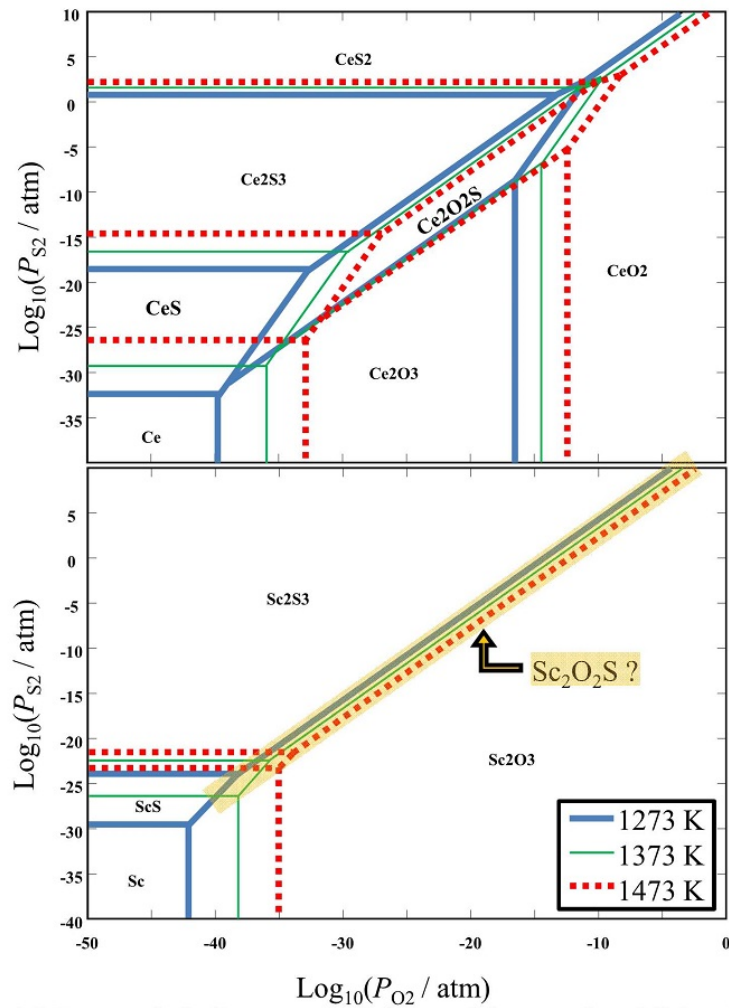
305 Therefore, almost single phase of  $\text{Sc}_2\text{S}_3$  with low oxygen concentration was successfully synthesized  
306 at 1473 K by using  $\text{CS}_2$  gas sulfurization technique. By controlling the feeding temperature of  $\text{CS}_2$   
307 liquid as low as 273 K, the carbon contamination could be minimized to 0.030 wt%C.

308

### 309 3.4 Transient phase of $\text{Sc}_2\text{O}_2\text{S}$

310 The formation of oxysulfides ( $\text{M}_2\text{O}_2\text{S}$  type) have been reported for most of IIIa group elements  
311 in the periodic table, *i.e.*,  $\text{M}=\text{Y}$  and rare earth metals from La to Lu [16, 26, 43-45]. The formation of  
312  $\text{Sc}_2\text{O}_2\text{S}$  was also reported in the mixture of  $\text{Sc}_2\text{O}_3$  and  $\text{Sc}_2\text{S}_3$  at 1773 K [28,29], by solidifying from  
313 the melt at 1873 K [29], or by sulfurization of  $\text{Sc}_2\text{O}_3$  in  $\text{H}_2\text{S}$  gas at 1823 K [21]. However, the  
314 thermochemical data on  $\text{Sc}_2\text{O}_2\text{S}$  has not been reported and compiled in the currently available  
315 database [16]. The stability diagram of the oxides and sulfides in Sc-O-S ternary system was plotted  
316 using only the available thermodynamic data [16]. As the first approach, the existence of  $\text{Sc}_2\text{O}_2\text{S}$  was  
317 neglected at all the temperatures as shown in Fig. 15, which could be due to the lack of data. When  
318 the temperature increases, the stable areas of metallic Sc and  $\text{Sc}_2\text{S}_3$  expand, and those of ScS and  
319  $\text{Sc}_2\text{O}_3$  shrink.

320



321

322 Fig.15 Potential diagram of the oxides and sulfides in the ternary Ce-O-S and Sc-O-S systems [16].

323

324 In synthesis of  $\text{Sc}_2\text{S}_3$ , the existence of  $\text{Sc}_2\text{O}_2\text{S}$  [28,29] was detected and ScS was never found in this

325 work. Because the stable region of ScS exists both at a very low partial pressure of sulfur ( $P_{\text{S}_2}$ ) and a

326 very low partial pressure of oxygen ( $P_{\text{O}_2}$ ) in Fig. 15, it is reasonable that ScS did not appear in a high

327  $P_{\text{S}_2}$  of  $\text{CS}_2$  gas environment. If  $\text{Sc}_2\text{O}_2\text{S}$  was thermodynamically stable phase, the stable region of

328  $\text{Sc}_2\text{O}_2\text{S}$  in Fig. 15 should exist at a boundary area between the regions of  $\text{Sc}_2\text{S}_3$  and  $\text{Sc}_2\text{O}_3$  (hatched

329 yellow area in Fig. 15). Hence, it is reasonable to refer to the stability region of  $\text{Ce}_2\text{O}_2\text{S}$  in the

330 Ce-O-S ternary system [16], where the phase boundaries between  $Ce_2O_3$  and  $Ce_2O_2S$  and, between  
331  $Ce_2O_2S$  and  $Ce_2S_3$  are parallel with that between  $Ce_2O_3$  and  $Ce_2S_3$ . Therefore, the stable region of  
332  $Sc_2O_2S$  can be drawn in a similar way for  $Ce_2O_2S$  if the thermodynamic values can be obtained.  
333 Because this work paid main attention in the synthesis of  $Sc_2S_3$ , the stability of  $Sc_2O_2S$  was not well  
334 studied due to lack of thermodynamic data. It will be separately reported.

335

#### 336 **4. Conclusion**

337 This study experimentally examined the sulfurization of  $Sc_2O_3$  by using  $CS_2$  gas to obtain  $Sc_2S_3$ .  
338 In conversion of  $Sc_2O_3$  to  $Sc_2S_3$ , the oxysulfide,  $ScO_2S$ , was found as an intermediate phase, and  
339 fairly stable at 1273 K. The optimum condition to synthesize almost pure phase of  $Sc_2S_3$  was to  
340 sulfurize  $Sc_2O_3$  at 1473 K by evaporating  $CS_2$  liquid at 273 K. The oxygen contamination was  
341 minimized to 2.22 wt%O. The reaction temperature and time directly affected the degree of  
342 sulfurization, and the carbon contamination remarkably increased by increasing the evaporation  
343 temperature of  $CS_2$  because of decomposition of  $CS_2$  to carbon and sulfur gas. The obtained  $Sc_2S_3$   
344 crystals showed the morphology of the hexagonal-shape plates. A practical method for producing a  
345 large amount of  $Sc_2S_3$  directly from the purified  $Sc_2O_3$  has been confirmed in this work. It is, then,  
346 expected to convert the oxide to pure metal Sc via  $Sc_2S_3$ , if calciothermic reduction or  
347 electrochemical reduction using molten salt can be applied.

348

349 **Acknowledgements**

350       The authors thank to Dr. Hirotaka Higuchi at Sumitomo Metal Mining Co., Ltd for his good  
351 discussion, and Mr. Nobuyuki Miyazaki for the technical supports of SEM observation at Office for  
352 the Promotion of Nanotechnology Collaborative Research, Hokkaido University. This work was  
353 financially supported in part by Grants-in-Aid from the Ministry of Education, Science and Sports  
354 (KAKENHI 17H0343409 and 18F1805409), the Japan Mining Industries Association, and  
355 Sumitomo Metal Mining Co., Ltd. The financial support of Japan Society for the Promotion of  
356 Science (JSPS) for research in Japan (Standard, P18054) is also acknowledged.

357

## 358 **References**

- 359 [1] Masahiro Murayama, Ryoji Kanno, Michihiko Irie, Shinya Ito, Takayuki Hata, Noriyuki  
360 Sonoyama, and Yoji Kawamoto, Synthesis of New Lithium Ionic Conductor Thio-LISICON Lithium  
361 Silicon Sulfides System, *J. Solid State Chem.*, 168, (2002) 140-148. DOI: 10.1006/jssc.2002.9701
- 362 [2] Atsushi Sawada, Akitoshi Hayashi, Masahiko Tatsumisago, Sulfide Solid Electrolyte with  
363 Favorable Mechanical Property for All-Solid-State Lithium Battery, *Sci. Rep.*, 3 (2013) 2261 1-5.  
364 DOI: 10.1038/srep02261
- 365 [3] C. Wood, A. Lockwood, J. Parker. A. Zoltan, D. Zoltan, A.R. Danielson, V. Raag, Thermoelectric  
366 properties of lanthanum sulfide, *J. Appl. Phys.*, 58 (1985) 1542-1547. DOI: 10.1063/1.336088
- 367 [4] H. Imai, Y. Shimakawa, and Y. Kubo, Large thermoelectric power factor in  $\text{TiS}_2$  crystal with  
368 nearly stoichiometric composition, *Phys. Rev. B*, 64 (2001) 241104 1-4. DOI:  
369 10.1103/PhysRevB.64.241104
- 370 [5] Michihiro Ohta, Shuhei Satoh, Toshihiro Kuzuya, Shinji Hirai, Masaru Kunii, Atsushi Yamamoto,  
371 Thermoelectric properties of  $\text{Ti}_{1+x}\text{S}_2$  prepared by  $\text{CS}_2$  sulfurization, *Acta Mater.*, 60 (2012), 7232-40.  
372 DOI: 10.1016/j.actamat.2012.09.035
- 373 [6] E. Guilmeau, A. Maignan, C. Wan and K. Koumoto, On the effects of substitution, intercalation,  
374 non-stoichiometry and block layer concept in  $\text{TiS}_2$  based thermoelectrics, *Phys. Chem. Chem. Phys.*  
375 17 (2015) 24541-24555. DOI: 10.1039/c5cp01795e
- 376 [7] Lanling Zhao, Xiaolin Wang, Frank Yun Fei, Jiyang Wang, Zhenxiang Cheng, Shixue Dou, Jun  
377 Wang and G. Jeffrey Snyder, High thermoelectric and mechanical performance in highly dense  
378  $\text{Cu}_{2-x}\text{S}$  bulks prepared by a melt-solidification technique, *J. Mater. Chem. A*, 18 (2015) 9432-9437.  
379 DOI: 10.1039/c5ta01667c
- 380 [8] Yuta Kikuchi, Yohan Bouyrie, Michihiro Ohta, Koichiro Suekuni, Makoto Aihara and Toshiro  
381 Takabatake, Vanadium-free colusites  $\text{Cu}_{26}\text{A}_2\text{Sn}_6\text{S}_{32}$  (A=Nb, Ta) for environmentally friendly  
382 thermoelectrics, *J. Mater. Chem. A.*, 4 (2016) 15207-15214. DOI: 10.1039/c6ta05945g
- 383 [9] M. Ohta, P. Jood, M. Murata, C-H. Lee, A. Yamamoto and H. Obara, An Integrated Approach to  
384 Thermoelectrics: Combining Phonon Dynamics, Nanoengineering, Novel Materials Development,  
385 Module Fabrication, and Metrology, *Adv. Energy Mater.*, 9 (23) (2019) 1801304. DOI:  
386 10.1002/aenm.201801304
- 387 [10] Nobuyoshi Suzuki, Shungo Natsui, Tatsuya Kikuchi and Ryosuke O. Suzuki, Reduction of  $\text{TiS}_2$   
388 By OS Process in  $\text{CaCl}_2$  Melt, *ECS Trans.*, 75 [15] (2016) pp.507-515. DOI:  
389 10.1149/07515.0507ecst
- 390 [11] Nobuyoshi Suzuki, Mariko Tanaka, Hiromi Noguchi, Shungo Natsui, Tatsuya Kikuchi, and  
391 Ryosuke O. Suzuki, Calcium Reduction of  $\text{TiS}_2$  in  $\text{CaCl}_2$  Melt, *Mater. Trans.*, 58 [3] (2017)  
392 pp.367-370. DOI: 10.2320/matertrans.MK201613
- 393 [12] Takahiro Matsuzaki, Shungo Natsui, Tatsuya Kikuchi, and Ryosuke O. Suzuki, Electrolytic

394 reduction of  $V_3S_4$  in molten  $CaCl_2$ , *Mater. Trans.*, 58 [3] (2017) pp.371-376. DOI:  
395 10.2320/matertrans.M2016305

396 [13] Eltefat Ahmadi, Yuta Yashima, Ryosuke O. Suzuki, and Sheikh Abdul Rezan, Formation of  
397 Titanium Sulfide from Titanium Oxycarbonitride by  $CS_2$  Gas, *Metal. Mater. Trans. B*, 49(4) (2018)  
398 1808-21. DOI: 10.1007/s11663-018-1278-8

399 [14] Changsheng Wu, Mingsheng Tan, Guozhu Ye, Derek J. Fray, and Xianbo Jin, High-Efficiency  
400 Preparation of Titanium through Electrolysis of Carbo-Sulfurized Titanium Dioxide, *ACS*  
401 *Sustainable Chem. Eng.*, 7 (2019) 8340-8346. DOI: 10.1021/acssuschemeng.8b06801

402 [15] Eltefat Ahmadi, and Ryosuke O. Suzuki, An innovative process for production of Ti metal  
403 powder via  $TiS_x$  from TiN, *Metal. Mater. Trans. B*, (2019), in press.  
404 doi:10.1007/s11663-019-01730-w.

405 [16] Antti Roine, HSC Chemistry, 8.0.8, Outotec Technologies, Pori, Finland (2014).

406 [17] M. Harata, T. Nakamura, H. Yakushiji and T. H. Okabe, Production of scandium and Al-Sc  
407 alloy by metallothermic reduction, *Journal Mineral Processing and Extractive Metallurgy*, 117 [2]  
408 (2008) 95-99. DOI: 10.1179/174328508X290876

409 [18] M. Harata, K. Yasuda, H. Yakushiji, T.H. Okabe, Electrochemical production of Al-Sc alloy in  
410  $CaCl_2$ - $Sc_2O_3$  molten salt, *J. Alloys Compd*, 474 (2009) 124-30. DOI: 10.1016/j.jallcom.2008.06.110

411 [19] Yong-Uk Han, Jae Woong Koh, Byong Pil Lee, Dong Joon Min, The dissolution mechanism of  
412  $Sc_2O_3$  in  $CaO$ - $CaCl_2$  flux for the calciothermic production of Al-Sc alloy, *J. Alloys Compd.*, 658  
413 (2016) 595-597. DOI: 10.1016/j.jallcom.2015.10.211

414 [20] Hiroaki Nakamura and Akira Kasahara, Electrical Conductivity of Solid Scandium Sulfide, *J.*  
415 *Japan Inst. Metals*, 50 [11] (1986) 974-979. DOI: 10.2320/jinstmet1952.50.11\_974

416 [21] J. P. Dismukes and J. G. White, The Preparation, Properties, and Crystal Structures of Some  
417 Scandium Sulfides in the Range  $Sc_2S_3$ -ScS, *Inorg. Chem.*, 3 [9] (1964) 1220-1228. DOI:  
418 10.1021/ic50019a004

419 [22] Wilhelm Klemm, Karl Meisel, Haus Ulrich von Vogel, Über die Sulfide der seltenen Erden, *Z.*  
420 *anorg, allgem. Chem.*, 190 (1), (1930) 123.

421 [23] R.F. Barrow and W. Jevons, The band spectrum of silicon monosulphide and its relation to the  
422 band spectra of similar molecules, *Proc. Roy. Soc. London A*, 169 (1939), 45-65. DOI:  
423 10.1098/rspa.1938.0194

424 [24] M. Skrobjan, N. Sato, T. Fujino, Preparation of neodymium sulphides by the reaction of  
425  $Nd_2(SO_4)_3$  with carbon disulphide, *J. Alloys Compd.*, 210 (1994), 291-297. DOI:  
426 10.1016/0925-8388(94)90152-X

427 [25] S. Hirai, K. Shimakage, Y. Saitou, T. Nishimura, Y. Uemura, M. Mitomo, L. Brewer, Synthesis  
428 and Sintering of Cerium(III) Sulfide Powders, *J. Am. Ceram. Soc.*, 81 (1) (1998), 145-51. DOI:  
429 10.1111/j.1151-2916.1998.tb02306.x

430 [26] H.A. Eick, The Preparation, Lattice Parameters and Some Chemical Properties of the Rare  
431 Earth Mono-thio Oxides, *J. Amer. Chem. Soc.*, 80 (1958) 43-44. DOI: 10.1021/ja01534a012

432 [27] Osvald Knop, Jean M. Hartley, Refinement of the Crystal Structure of Scandium Oxide, *Can. J.*  
433 *Chem.*, 46 (1968) 1446-1450. DOI: doi.org/10.1139/v68-236

434 [28] M. Julien-Pouzol, S. Jaulmes, M. Guittard, P. Laruelle, Oxysulfure de scandium  $\text{Sc}_2\text{O}_2\text{S}$ , *J. Sol.*  
435 *Stat. Chem.*, 26 [2] (1978) 185-188. DOI: 10.1016/0022-4596(78)90150-0

436 [29] V. Brozek, J. Flahaut, M. Guittard, M. Julien-Pouzol, and M. P. Pardo, Chalcogen Derivatives of  
437 Scandium, *Bull. Soc. Chim. Fr., Part. I*, 9-10 (1974) 1740-1742.

438 [30] H. Jedlicka, H. Nowotny, F. Benesovsky, Zum System Scandium-Kohlenstoff, 2. Mitt.:  
439 Kristallstruktur des C-reichen Carbids, *Monatsh. Chem.*, 102 (1971) 389-403. DOI:  
440 10.1007/BF00909332

441 [31] Bohumil Hájek, Pavel Karen, Vlastimil Brožek, Studies on Hydrolysable Carbides XX: the  
442 Hydrolysis of the Scandium Carbide  $\text{Sc}_{15}\text{C}_{19}$ , *J. Less-Comm. Metals*, 96 (1984) 35-48. DOI:  
443 10.1016/0022-5088(84)90177-2

444 [32] Bohumil Hájek, Pavel Karen, Vlastimil Brožek, Studies on Hydrolysable Carbides. XXII: the  
445 Carbothermal Reduction of Scandium Oxide  $\text{Sc}_2\text{O}_3$ , *Monatsh. Chem. Chem. Month.*, 117 (1986)  
446 1271-1278. DOI: 10.1007/BF00810872

447 [33] Helga Auer-Welsbach and H. Nowotny, Zur Frage des Scandiumcarbids, *Monatsh. Chem.*, 92  
448 (1961) 198-201. DOI:10.1007/BF00914086

449 [34] H. Nowotny and Helga Auer-Welsbach, Über das Scandiumcarbid, *Monatsh. Chem.*, 92 (1961)  
450 789-793. DOI: 10.1007/BF00918639

451 [35] H. Rassaerts, H. Nowotny, G. Vinek and F. Benesovsky, Zum System Scandium-Kohlenstoff, 1.  
452 Mitt.: *Monatsh. Chem.*, 98 (1967) 460-468. DOI: 10.1007/BF00899965

453 [36] N.H. Krikorian, A.L. Giorgi, E.G. Szklarz, M.C. Krupka and B.T. Matthias, Preparation and  
454 Superconductivity of Germanium-Stabilized  $\text{Sc}_{13}\text{C}_{10}$ , *J. Less-Comm. Met.*, 19 (1969) 253-257. DOI:  
455 10.1016/0022-5088(69)90101-5

456 [37] F. Petru, Über das Scandiumdicarbid  $\text{ScC}_2$ , *Z. Chem.*, 9 [2] (1969) 71-72.

457 [38] F. Petru, Sur les carbures de scandium, *Rev. de Chem. Minerale*, 7 [3] (1970) 515-

458 [39] Rainer Pöttgen, Wolfgang Jeitschko,  $\text{Sc}_3\text{C}_4$ , a Carbide with  $\text{C}_3$  Units Derived from Propadiene,  
459 *Inorg. Chem.*, 30 (1991) 427-431. DOI: 10.1021/ic00003a013

460 [40] Roald Hoffmann, H.-Jürgen Meyer, The Electronic Structure of Two Novel Carbides,  $\text{Ca}_3\text{Cl}_2\text{C}_3$   
461 and  $\text{Sc}_3\text{C}_4$ , Containing  $\text{C}_3$  Units, *Z. anorg. Allg. Chem.*, 607 (1992) 57-71. DOI:  
462 10.1002/zaac.19926070112

463 [41] Erick A. Juarez-Arellano, Björn Winkler, Lkhamsuren Bayarjargal, Alexandra Friedrich, Victor  
464 Milman, Daniel R. Kammler, Simon M. Clark, Jinyuan Yan, Monika Koch-Müller, Florian Schröder,  
465 Miguel Avalos-Borja, Formation of scandium carbides and scandium oxycarbide from the elements

466 at high- $(P,T)$  conditions, *J. Sol. Stat. Chem.*, 183 (2010) 975-983. DOI: 10.1016/j.jssc.2010.02.019  
467 [42] Erick A. Juarez-Arellano, Björn Winkler, Sven C. Vogel, Anatoliy Senyshyn, Daniel R.  
468 Kammler, Miguel Avalos-Borja, In situ observation of the reaction of scandium and carbon by  
469 neutron diffraction, *J. Alloys Compds.*, 509 (2011) 1-5 DOI: 10.1016/j.jallcom.2010.08.081.  
470 [43] C. Sourisseau, R. Cavagnat, R. Mauricot, F. Boucher, M. Evain, Structure and bondings in  
471 cerium oxysulfide compounds. I - Electronic, infrared and resonance Raman spectra of  $Ce_{2.0}O_{2.5}S$ , *J.*  
472 *Raman Spectroscopy*, 28 [12] (1997) 965-971. DOI:  
473 10.1002/(SICI)1097-4555(199712)28:12<965::AID-JRS191>3.0.CO;2-D  
474 [44] L.E. Sobon, K.A. Wickersheim, R.A. Buchanan, R.V. Alves, Growth and Properties of  
475 Lanthanum Oxysulfide Crystals, *J. Appl. Phys.*, 42 (1971) 3049-3053. DOI: 10.1063/1.1660682  
476 [45] M. Leskelä, L. Niinistö, Thermal Decomposition of Rare Earth Oxysulfides in Air, *J. Therm.*  
477 *Analy.*, 18, (1980) 307-314. DOI: 10.1007/BF02055815  
478  
479

## 480 **Figure Captions**

481 Fig.1 A schematic illustration of the experimental setup.

482 Fig.2 Mass change after CS<sub>2</sub> gas sulfurization for 7.2 ks.

483 Fig.3 Mass change after CS<sub>2</sub> gas sulfurization.

484 Fig.4 Apparent view of sulfurized sample at 1473 K for 7.2 ks. CS<sub>2</sub> liquid was hold at 273 K (a), and

485 313 K (b).

486 Fig. 5 X-ray diffraction patterns of the samples sulfurized at various temperatures for 7.2 ks.

487 Fig.6 X-ray diffraction patterns of the samples sulfurized at 1373 K.

488 Fig.7 Sulfur content of the sulfurized samples.

489 Fig.8 The residual oxygen content of the sulfurized samples.

490 Fig. 9 SEM images of (a) as-received scandium oxide and the synthesized sulfides at 1273 K (b, c),

491 and 1473 K (d, e) for 10.8 ks.

492 Fig.10 Mass change of sulfurized samples for 7.2 ks at various CS<sub>2</sub> evaporation temperatures.

493 Fig. 11 Oxygen concentration of the sulfurized samples for 7.2 ks at various CS<sub>2</sub> evaporation

494 temperatures.

495 Fig.12 Vapor pressure of CS<sub>2</sub> vs evaporation temperature [16].

496 Fig.13 Carbon content of the samples prepared by evaporation of CS<sub>2</sub> at various temperatures.

497 Fig.14 XRD pattern of sulfurized sample at 1473 K for 7.2 ks by using CS<sub>2</sub> gas evaporated at 313 K.

498 Fig.15 Potential diagram of the oxides and sulfides in the ternary Ce-O-S and Sc-O-S systems [16].

499